

**SYNTHESIS OF FREE STANDING ANODIC ZrO<sub>2</sub> NANOTUBES IN  
POTASSIUM CARBONATE/ETHYLENE GLYCOL ELECTROLYTE  
FOR PHOTOCATALYST APPLICATION**

**by**

**NURUL IZZA SOAID**

**Thesis submitted in fulfilment of the  
requirements for the degree of  
Master of Science**

**June 2019**

## ACKNOWLEDGEMENT

Alhamdulillah, all praises to Allah SWT for His blessing to complete this study.

Firstly, I would like to express my sincere gratitude to my supervisor, Assoc. Prof. Dr. Zainovia Lockman for the continuous support of my MSc study and related research, for her guidance, encouragement, patience, and immense knowledge. Her guidance helped me in all the time of research and writing of this thesis.

I also would like to thank staff of School of Materials and Mineral Resources Engineering especially to Mohd Azzam Rejab who in charge Electronic Lab for being helpful and kind, Encik Kemuridan Md. Desa, Encik Mohammad Azrul Zainol Abidin, Encik Abdul Rashid Selamat, Encik Khairi Khalid, Puan Haslina Zulkifli, who gave access to the laboratory and research facilities. Without they precious support it would not be possible to conduct this research. To my GEMS Group, thanks for your help started from the beginning till the end especially; Monna Rozana, Nurulhuda Bashrom, Nyein Nyein, Mustafa Ali Azhar Taib, Chan Yihoong, and Faisal Budiman.

Finally, I would like to express special gratitude to my beloved mom, Mahani Man, for her pray, unconditional love and especially for financial support through this journey. I also thank to my sister; Fatin Syafirah Soaid, my uncles and aunt; Ibrahim Othman, Abdul Jalil Man, Zarita Mat; and last but not least Anas Amirul Ahmad Annuar, for their love and kindness.

Last but not least, my thanks go to all the people who have supported me to complete the research work directly or indirectly.

## TABLES OF CONTENTS

	<b>Page</b>
<b>ACKNOWLEDGEMENT</b>	ii
<b>TABLE OF CONTENTS</b>	iii
<b>LIST OF TABLES</b>	vi
<b>LIST OF FIGURES</b>	vii
<b>LIST OF ABBREVIATIONS</b>	xiii
<b>LIST OF SYMBOLS</b>	iv
<b>ABSTRAK</b>	xv
<b>ABSTRACT</b>	xvi
<b>CHAPTER ONE : INTRODUCTION</b>	
1.1 Background	1
1.2 Problem statements	5
1.3 Objectives	8
1.4 Research scope	9
1.5 Outline of thesis	9
<b>CHAPTER TWO : LITERATURE REVIEW</b>	
2.1 Introduction	11
2.2 Few methods to synthesize ZrO <sub>2</sub>	11
2.3 Anodisation of Zirconium	14
2.3.1 Evolution of ZrO <sub>2</sub> in anodisation process	14
2.3.2 Electrolyte effect on formation of ZNTs	17
2.3.2 (a) Glycerol-based electrolyte	18
2.3.2 (b) Ethylene Glycol-based electrolyte	22
2.3.2 (c) Buffered electrolyte	23
2.3.3 Synthesis of Free-standing ZrO <sub>2</sub> nanotubes	33
2.3.4 Properties of ZrO <sub>2</sub> nanotubes	35
2.4 Photocatalysis of ZrO <sub>2</sub> Nanotubes/Nanostructures	40

### **CHAPTER THREE : RAW MATERIALS AND RESEARCH METHODOLOGY**

3.1	Introduction	45
3.2	Raw materials and chemical	45
3.3	Experimental procedure	47
	3.3.1 Anodisation process	48
	3.3.2 Annealing process	50
	3.3.3 Photocatalytic activity of methyl orange degradation	51
3.4	Characterization technique	52
	3.4.1 Morphology study	52
	3.4.2 Crystallinity	54
	3.4.3 Surface analysis	54
	3.4.4 Optical property	55
	3.4.5 Degradation measurement of MO	55

### **CHAPTER FOUR : RESULTS AND DISCUSSION**

4.1	Introduction	56
4.2	Evolution of ZrO <sub>2</sub> Nanotubes in EG electrolyte	56
	4.2.1 EG/NH <sub>4</sub> F with water addition (EG/NH <sub>4</sub> F/H <sub>2</sub> O)	61
	4.2.2 EG/NH <sub>4</sub> F with hydrogen peroxide (EG/NH <sub>4</sub> F/H <sub>2</sub> O <sub>2</sub> )	72
	4.2.3 EG/NH <sub>4</sub> F with potassium carbonate addition (EG/NH <sub>4</sub> F/K <sub>2</sub> CO <sub>3</sub> )	79
	4.2.3 (a) 0.5 M of K <sub>2</sub> CO <sub>3</sub> addition	80
	4.2.3 (b) 1 M of K <sub>2</sub> CO <sub>3</sub> addition	87
	4.2.3.(c) 3 M of K <sub>2</sub> CO <sub>3</sub> addition	92
4.3	Self-peeling mechanism	97
	4.3.1 Different anodisation voltage on formation of ZrO <sub>2</sub> Nanotubes	101
	4.3.2 Different wt % of NH <sub>4</sub> F addition in electrolyte	109
4.4	Annealing process of ZrO <sub>2</sub> nanotubes	113

4.4.1	Morphology free-standing ZrO <sub>2</sub> nanotubes after annealing process	113
4.4.2	Crystallinity study of ZrO <sub>2</sub> nanotubes	117
4.4.3	Optical properties of free-standing ZNTs in different annealing temperature	120
4.4.4	Surface properties of free-standing ZNTs	122
4.5	Study of photocatalytic properties	124
4.5.1	Photocatalytic study	124

## **CHAPTER FIVE : CONCLUSION AND RECOMMENDATION**

5.1	Conclusion	126
5.2	Recommendation	128

<b>REFERENCES</b>	<b>129</b>
-------------------	------------

## **PUBLICATION**

## LIST OF TABLES

		Page
Table 2.1	Summary of anodization condition on formation of ZrO <sub>2</sub> .	26
Table 2.2	Comparison of ZrO <sub>2</sub> nanostructures for degradation of methyl orange	44
Table 3.1	Raw materials and chemicals used in anodization process and photoinduced study.	46
Table 4.1	Summary of ZNTs length in different addition of oxidant in electrolyte.	97

## LIST OF FIGURES

		Page
Figure 1.1	Overview flow of free-standing ZNTs used in degradation of dye	4
Figure 2.1	SEM micrographs of anodised zirconium: a) surface and b) cross-section view of porous structures made in 1 M H <sub>2</sub> SO <sub>4</sub> / 0.1 wt% NH <sub>4</sub> F (Tsuchiya and Schmuki, 2004), c) surface and d) cross-section view of nanotubes structures made in 0.5 wt% of NH <sub>4</sub> F in 1 M (NH <sub>4</sub> ) <sub>2</sub> SO <sub>4</sub> (Tsuchiya et al., 2005c).	16
Figure 2.2	Photographs of a) the detachments of anodic ZrO <sub>2</sub> nanotubes layer from the underlying Zr metal, (b) a freestanding ZrO <sub>2</sub> membrane (Shin and Lee, 2009).	33
Figure 2.3	Photographs of freestanding ZrO <sub>2</sub> membrane by using a) chemical etching (Fang et al., 2011), (b) potential shock method (Fang et al., 2012a).	34
Figure 2.4	XRD spectra of ZrO <sub>2</sub> nanotubes at different annealing temperature Zhao et al. (2008a).	36
Figure 2.5	SEM images of ZrO <sub>2</sub> nanotubes annealed at different temperature: a) 200 ° C, b) 400, c) 600 and d) 800 ° C (Guo et al., 2009c).	37
Figure 2.6	FTIR spectra of ZrO <sub>2</sub> nanotubes of: a) as-anodized, annealed at: b) 200, 400, 600 and 800 ° C.	38
Figure 2.7	PL spectra of ZrO <sub>2</sub> nanotubes: a) as-anodized and b) annealed at 400 ° C (Fang et al., 2013).	39
Figure 2.8	Proposed mechanism of MO degradation on tetragonal ZrO <sub>2</sub> (Adapted from Reddy et al. (2018).	41
Figure 2.9	Structure of methyl orange	42
Figure 3.1	Overall flow chart of the experimental procedure.	47
Figure 3.2	Flow chart of anodisation process.	49
Figure 3.3	Anodisation setup of ZrO <sub>2</sub> .	50
Figure 3.4	Heating profile of thermal annealing of self-peeling ZrO <sub>2</sub> nanotubes.	50

Figure 3.5	Experimental set up for degradation of methyl orange.	51
Figure 4.1	FESEM images of surface of as-anodized ZrO <sub>2</sub> nanostructures formed in EG/NH <sub>4</sub> F electrolyte for 1 H at different voltage (a) 20 V, (b) 40 V, (c) 60 V and (d) cross-section at 60 V.	57
Figure 4.2	TEM image of ZrO <sub>2</sub> nanostructures formed in EG/NH <sub>4</sub> F electrolyte for 1 H at 60 V.	58
Figure 4.3	Current density - time curves for anodization of ZrO <sub>2</sub> nanostructures formed in EG/NH <sub>4</sub> F electrolyte for 1 H at different voltage.	60
Figure 4.4	FESEM images of surface and cross-section of as-anodized ZNTs formed in EG/NH <sub>4</sub> F electrolyte for 1 H at different vol % of H <sub>2</sub> O (a) 0.5 vol %, (b) 1 vol %, (c) 2 vol %, (d) 3 vol % and (e) 4 vol %.	62
Figure 4.5	EDX analysis of ZrO <sub>2</sub> nanostructures formed in EG/NH <sub>4</sub> F electrolyte for 1 H at 60 V in 0.5 vol % of H <sub>2</sub> O added.	64
Figure 4.6	TEM image of ZrO <sub>2</sub> nanostructures formed in EG/NH <sub>4</sub> F electrolyte for 1 H at 60 V in different vol % of H <sub>2</sub> O a) 0.5 vol %, b) 1 vol % and c) 3 vol %.	65
Figure 4.7	Current density - time curves for anodization of ZrO <sub>2</sub> nanostructures in different vol % of H <sub>2</sub> O addition in electrolyte.	66
Figure 4.8	TEM images of bottom part of ZrO <sub>2</sub> nanostructures formed in EG/NH <sub>4</sub> F electrolyte for 1 H at 60 V in 0.5 vol % of H <sub>2</sub> O added.	67
Figure 4.9	Schematic diagram on formation of ZNTs by anodization.	70
Figure 4.10	Photograph images of as-anodized ZrO <sub>2</sub> nanostructures formed in EG/NH <sub>4</sub> F electrolyte for 1 H at different vol % of H <sub>2</sub> O.	73
Figure 4.11	FESEM images of surface and cross-section of as-anodized ZNTs formed in EG/NH <sub>4</sub> F electrolyte for 1 H at different vol % of H <sub>2</sub> O <sub>2</sub> (a) 0.5 vol %, (b) 1 vol %, (c) 2 vol %, (d) 3 vol % and (e) 4 vol %.	75
Figure 4.12	TEM image of ZNTs formed in EG/NH <sub>4</sub> F electrolyte for 1 H at 60 V in different vol % of H <sub>2</sub> O <sub>2</sub> a) 0.5 vol %, b) 1 vol % and c) 3 vol %.	76



Figure 4.13	Photograph images of as-anodized ZNTs formed in EG/NH <sub>4</sub> F electrolyte for 1 H at different vol % of H <sub>2</sub> O <sub>2</sub> .	76
Figure 4.14	EDX analysis of ZNTs formed in EG/NH <sub>4</sub> F electrolyte for 1 H at 60 V in 0.5 vol % of H <sub>2</sub> O <sub>2</sub> added.	76
Figure 4.15	Photograph images of as-anodized ZNTs formed in EG/NH <sub>4</sub> F/H <sub>2</sub> O <sub>2</sub> after immersion in electrolyte for 24 H.	77
Figure 4.16	Current density - time curves for anodization of ZNTs in different vol% of H <sub>2</sub> O <sub>2</sub> addition in electrolyte.	78
Figure 4.17	FESEM images of surface and cross-section of as-anodized ZNTs formed in EG/NH <sub>4</sub> F electrolyte for 1 H at different vol % of 0.5 M K <sub>2</sub> CO <sub>3</sub> addition (a) 0.5 vol %, (b) 1 vol %, (c) 2 vol %, (d) 3 vol % and (e) 4 vol %.	82
Figure 4.18	EDX analysis of ZNTs formed in EG/NH <sub>4</sub> F electrolyte for 1 H at 60 V in 0.5 vol % of 0.5 M K <sub>2</sub> CO <sub>3</sub> added.	83
Figure 4.19	TEM image of ZNTs formed in EG/NH <sub>4</sub> F electrolyte for 1 H at 60 V in 0.5 M K <sub>2</sub> CO <sub>3</sub> addition: a) 0.5 vol %, b) 1 vol % and c) 3 vol %.	84
Figure 4.20	Photograph images of as-anodized ZNTs formed in EG/NH <sub>4</sub> F electrolyte for 1 H at different vol % of 0.5 M K <sub>2</sub> CO <sub>3</sub> .	86
Figure 4.21	Current density - time curves for anodization of ZNTs in different vol% of 0.5 M K <sub>2</sub> CO <sub>3</sub> addition in electrolyte.	86
Figure 4.22	FESEM images of surface and cross-section of as-anodized ZNTs formed in EG/NH <sub>4</sub> F electrolyte for 1 H at different vol % of 1 M K <sub>2</sub> CO <sub>3</sub> addition (a) 0.5 vol %, (b) 1 vol %, (c) 2 vol %, (d) 3 vol % and (e) 4 vol %.	88
Figure 4.23	TEM image of ZNTs formed in EG/NH <sub>4</sub> F electrolyte for 1 H at 60 V in different vol % of 1 M K <sub>2</sub> CO <sub>3</sub> a) 0.5 vol %, b) 1 vol % and c) 3 vol %.	89

Figure 4.24	Photograph images of as-anodized ZNTs formed in EG/NH <sub>4</sub> F electrolyte for 1 H at different vol % of 1 M K <sub>2</sub> CO <sub>3</sub> .	90
Figure 4.25	Current density - time curves for anodization of ZNTs in different vol% of 1 M K <sub>2</sub> CO <sub>3</sub> addition in electrolyte.	91
Figure 4.26	FESEM images of surface and cross-section of as-anodized ZNTs formed in EG/NH <sub>4</sub> F electrolyte for 1 H at different vol % of 3 M K <sub>2</sub> CO <sub>3</sub> addition (a) 0.5 vol %, (b) 1 vol %, (c) 2 vol %, (d) 3 vol % and (e) 4 vol %.	93
Figure 4.27	TEM image of ZNTs formed in EG/NH <sub>4</sub> F electrolyte for 1 H at 60 V in 1 vol % of 3 M K <sub>2</sub> CO <sub>3</sub> addition.	94
Figure 4.28	Photograph images of as-anodized ZNTs formed in EG/NH <sub>4</sub> F electrolyte for 1 H at different vol % of 3 M K <sub>2</sub> CO <sub>3</sub> .	96
Figure 4.29	Current density - time curves for anodization of ZNTs in different vol% of 3 M K <sub>2</sub> CO <sub>3</sub> addition in electrolyte.	98
Figure 4.30	Self-peeling mechanism of ZNTs.	99
Figure 4.31	EDX mapping of as-anodised sample of 1 vol % of 1 M K <sub>2</sub> CO <sub>3</sub> addition in EG + NH <sub>4</sub> F electrolyte at 60 V for 1 H.	101
Figure 4.32	FESEM images (cross-section) of as-anodized ZNTs formed in EG/NH <sub>4</sub> F electrolyte for 1 H at different voltage of 1 M of K <sub>2</sub> CO <sub>3</sub> addition (a) 20 V, (b) 40 V, (c) 60 V, (d) 80 V, (e) 100 V, (f) 120 V, (g) 140 V and (h) 160 V.	103
Figure 4.33	FESEM images (surface) of as-anodized ZNTs formed in EG/NH <sub>4</sub> F electrolyte for 1 H at different voltage of 1 M of K <sub>2</sub> CO <sub>3</sub> addition (a) 20 V, (b) 40 V, (c) 60 V, (d) 80 V, (e) 100 V, (f) 120 V, (g) 140 V and (h) 160 V.	104
Figure 4.34	EDX analysis of ZrO <sub>2</sub> nanostructures formed in EG/NH <sub>4</sub> F electrolyte for 1 H at 120 V in 1 vol % of 1 M K <sub>2</sub> CO <sub>3</sub> added.	105
Figure 4.35	TEM image of ZNTs formed in EG/NH <sub>4</sub> F electrolyte for 1 H in 1 vol % of 1 M K <sub>2</sub> CO <sub>3</sub> a) 60 %, b) 80 V, c) 120 V and d) 160 V.	106

Figure 4.36	Photograph images of electrolyte after anodization process at different voltages: a) 60 V, b) 140 V and c) 160 V.	107
Figure 4.37	Current density - time curves for anodization of ZNTs in different voltage of 1 M $K_2CO_3$ addition in electrolyte.	108
Figure 4.38	FESEM images of surface and cross-section of as-anodized ZNTs formed in EG/1M $K_2CO_3$ electrolyte for 1 H at different w % of $NH_4F$ addition (a) 0.05 w %, (b) 0.1 w %, (c) 0.2 w %, (d) 0.3 w %, (e) 0.4 w % and (f) 0.5 w %.	110
Figure 4.39	Photograph images of as-anodized ZNTs formed in EG/1 M $K_2CO_3$ for 1 H at different w % of $NH_4F$ .	111
Figure 4.40	Current density - time curves for anodization of ZNTs in different w% of $NH_4F$ addition in electrolyte.	112
Figure 4.41	FESEM images of surface and cross-section of as-annealed ZNTs formed in EG/1M $K_2CO_3$ electrolyte for 1 H at different annealing temperature (a,b) 200 ° C, (c,d) 400 ° C, (e,f) 600 ° C, and (g,h) 800 ° C.	114
Figure 4.42	Morphology transformation of ZNTs as different annealing temperature.	115
Figure 4.43	a) HRTEM image and corresponding EDS mapping images of b) Zr, c) O, d) F and e) EDS spectrum of ZNTs at 800 ° C annealing temperature.	116
Figure 4.44	Photograph images of SP-ZONs after annealing at different temperature: a) 200 ° C, (b) 400 ° C, (c) 600 ° C, and (d) 800 ° C.	117
Figure 4.45	XRD patterns of SP-ZONs at different annealing temperature.	118
Figure 4.46	HRTEM image (inset shows SAED pattern) of as-anodized SP-ZONs.	118
Figure 4.47	SAED patterns of SP-ZONs annealing at (a) 600 and (b) 800 ° C.	121
Figure 4.48	PL spectra of: (a) SP-ZONs as-anodized and annealed at different temperature, (b) Xe lamp emission (Presciutti et al., 2014).	122

Figure 4.50	FTIR spectra of SP-ZONs: a) as-anodized sample, b) annealed at different temperature.	122
Figure 4.51	Degradation of methyl orange of annealed ZNTs at different temperature for 1 vol % of 1 M $K_2CO_3$ addition.	125

## LIST OF ABBREVIATIONS

AOPs	Advanced oxidation processes
ACA	Acetylacetone
EG	Ethylene glycoll
LAHC	Laurylamine hydrocholide
M	Metal
MO	Metyl orange
MOx	Metal oxide
ZNTs	Zirconia nanotubes
ZP	Zirconium (IV) propoxide

## LIST OF SYMBOLS

h	Hour
M	Molar
vol	Volume
%	Percentage
° C	Degree celcius
Cl <sup>-</sup>	Chloride ion
•OH	Hydroxyl radical
OH <sup>-</sup>	Hydroxyl ion
n	Number
e <sup>-</sup>	Electron
M <sup>n+</sup>	Metal ion
O <sup>2-</sup>	Oxide ion

**SINTESIS ANODIK TIUB NANO  $ZrO_2$  BEBAS BERDIRI DALAM  
KALIUM KARBONAT/ETILENA GLIKOL ELEKTROLIT BAGI  
APLIKASI PEMANGKIN CAHAYA**

**ABSTRAK**

Tiub nano  $ZrO_2$  berjaya di sintesis menggunakan kaedah penganodan. Campuran etilena glikol (EG) dengan ammonium fluorit ( $NH_4F$ ) menghasilkan struktur morfologi seperti karang  $ZrO_2$ . Kekurangan oksigen di dalam elektrolit menghadkan pertumbuhan tiub nano  $ZrO_2$  dalam kaedah penganodan. Oleh sebab itu, tambahan larutan kalium karbonat ( $K_2CO_3$ ) sebagai penyedia oksigen dalam elektrolit penganodan meningkatkan pertumbuhan struktur berliang  $ZrO_2$  kepada struktur tiub nano. Penambahan jumlah larutan  $K_2CO_3$  dari 0.5 vol % kepada 4 vol % dalam elektrolit penganodan, panjang tiub nano meningkat dalam 60 ke 80 nm. Selain itu, penambahan  $K_2CO_3$  membawa kepada pembentukan serpihan  $ZrO_2$  yang dipanggil nyahlekatan  $ZrO_2$ . Nyahlekatan  $ZrO_2$  ini dicapai dalam jangka masa yang lebih pendek berbanding kerja lain. Kelebihan nyahlekatan  $ZrO_2$  boleh digunakan sebagai pemangkin untuk rawatan sisa air seperti aplikasi pemangkin foto. Dalam kerja ini, nyahlekatan  $ZrO_2$  digunakan untuk menilai aktiviti pemangkin foto terhadap metil oren (MO). Hasilnya telah dibandingkan dengan sampel penyepuhlidapan nyahlekatan  $ZrO_2$ . Suhu penyepuhlidapan di kaji dalam julat 200, 400 600 dan 800 °C. Sampel asal penganodan menunjukkan penguraian terbaik sekitar 70 % berbanding dengan sampel penyepuhlidapan hanya mengurai sekitar 40 %.

# **SYNTHESIS OF FREE STANDING ANODIC ZrO<sub>2</sub> NANOTUBES IN POTASSIUM CARBONATE/ETHYLENE GLYCOL ELECTROLYTE FOR PHOTOCATALYST APPLICATION**

## **ABSTRACT**

ZrO<sub>2</sub> nanotubes were successfully synthesis by using anodisation method. Mixture of ethylene glycol (EG) with ammonium fluoride (NH<sub>4</sub>F) produced coral-like structures morphology of ZrO<sub>2</sub>. Lack of oxygen provider in electrolyte limit the growth of ZrO<sub>2</sub> nanotubes using anodisation method. Therefore, addition potassium carbonate (K<sub>2</sub>CO<sub>3</sub>) solution as oxygen provider in the anodic electrolyte enhanced the growth of ZrO<sub>2</sub> porous structure to nanotubular structure. Increasing from 0.5 vol % to 4 vol % of K<sub>2</sub>CO<sub>3</sub> in anodic electrolyte, the length of nanotubes increased from 8 to 20 μm as the K<sub>2</sub>CO<sub>3</sub> in anodic electrolyte. Average diameter of the ZrO<sub>2</sub> nanotubes about 60 to 80 nm. Besides, addition of K<sub>2</sub>CO<sub>3</sub> lead to the formation of loose ZrO<sub>2</sub> flakes as so-called free-standing ZrO<sub>2</sub>. The free-standing ZrO<sub>2</sub> achieved by shorter time frame compared to others work. The advantages of free-standing ZrO<sub>2</sub> can be used as catalyst for wastewater treatment such as photocatalyst application. In this work, as anodised free-standing ZrO<sub>2</sub> were used to evaluate its photocatalytic activity towards methyl orange (MO). The results were compared with annealed free-standing ZrO<sub>2</sub>. The annealing temperature studied is in the range of 200 to 800 °C. As-anodised samples showed the best degradation which around 70 % compared to anneal samples only degraded around 40 %





## CHAPTER ONE

### INTRODUCTION

#### 1.1 Background

Water is essential to human, plant and animal. Even though our planet is covered by 75 % of water, only about 3 % is suitable for drinking. Water has been widely used for industries, for production of energy and in agricultural activities. Since the world population is increasing, human will start to suffer when the demand to get fresh water increasing from time to time (Rodell, Famiglietti et al. 2018). This will become worse due to rapid industrial activities, and environmental pollution which is occurring at an alarming rate. As a result, contamination of water is regarded as one of the most severe global problems.

Pollution of water comes by industry such as textile and fabric industries whereby high amount of organic dyes are released to the water bodies before proper treatment. Textile dyes are substances that can be used to colour fabrics and when the dyes are soaked onto the fabrics, the fabrics will be permanently coloured. There are many different types of dyes for specific colouration and applications (Sha, Mathew et al. (2016)). During the colouring process, improper procedures generate large amounts of dyes residues. If not being treated, it will be directly released into water bodies like river or sea. Among the residues of dyes that pollute environment, azo dyes have been reported to be discharged in large quantities. Azo dyes are toxic substance and some of them can induce genotoxicity and mutagenicity (de Campos Ventura-Camargo and Marin-Morales 2013). Methyl orange (MO) is an example of azo dye which is extensively used in the textile industry but it is not biodegradable. Methods to treat MO dyes before discharged to water bodies are therefore needed.

Advanced oxidation processes (AOPs) are example of effective wastewater treatment method. AOPs is defined by Glaze, Kang et al. (1987) as a process of treatment that generate oxidizing agent like hydroxyl radicals ( $\bullet\text{OH}$ ) which can be performed at room temperature and its able to oxidize pollutants in contaminated water to less harmful substances. AOPs consist of several methods such as Fenton method, ozonation, photocatalysis, and cavitation. AOP process can be applied in oxidizing azo dyes to less harmful substances (Oturán and Aaron 2014).

Among the listed AOP methods, photocatalysis is preferred due to its effectiveness and simplicity. In this process, a semiconductor material is required. Illumination of light may produce photons that are required for the electron-hole pair formation. Once the energy of photon is greater or equal to its band gap, electron-hole pairs can be form. Holes react with hydroxyl ion ( $\text{OH}^-$ ) from the wastewater to produce  $\bullet\text{OH}$ .  $\bullet\text{OH}$  is one of the most powerful oxidizing agents which able to react instantaneously with the Azo dyes in its vicinity and disintegrate into  $\text{CO}_2$  and  $\text{H}_2\text{O}$  molecules which are nontoxic.

Choosing the right semiconductor material is therefore crucial since there are certain properties needed for a material to behave as catalyst in photocatalysis process. Titanium dioxide ( $\text{TiO}_2$ ) has been widely used as catalyst for the photocatalysis process because it has high photocatalytic activity, low cost, resistance to photo corrosion, favourable band-gap energy and non-toxicity reviewed by Linsebigler, Lu et al. (1995). Other materials that can act as suitable catalyst in photocatalysis process are  $\text{ZnO}$ ,  $\text{CuO}$ ,  $\text{WO}_3$  and  $\text{ZrO}_2$ .

ZrO<sub>2</sub> is considered as an interesting alternative of TiO<sub>2</sub> since it can be excited to produce electron-hole pairs. ZrO<sub>2</sub> is a typical ceramic material. Three types of ZrO<sub>2</sub> are known to exist which are cubic, tetragonal, and monoclinic. ZrO<sub>2</sub> can be synthesized with different chemical compositions depending on the method of preparation. ZrO<sub>2</sub> has many useful applications such as solid oxide fuel cell (Kim, Kim et al. (2014)), oxygen sensor (Fidelus, Zhou et al. (2015)), and catalyst (Witoon, Chalorngham et al. (2016)) with excellent surface properties. However, not many studies have been reported on the use of ZrO<sub>2</sub> as photocatalyst to degrade azo dyes. ZrO<sub>2</sub> has been applied as catalyst because of its acid-based surface properties, high chemical stability, and hydrophilicity. In this work, photocatalytic properties of ZrO<sub>2</sub> were studied. ZrO<sub>2</sub> was fabricated in a form of nanotubular structure by anodisation of zirconium foil.

Anodisation is a method to grow thin oxide film on a metal substrate with the presence of electrolyte. Oxidation reaction happened at the metal (M) when it is exposed to high applied voltage and may release M<sup>n+</sup> ions and electrons (Equation 1.1). M<sup>n+</sup> ions will react with O<sup>2-</sup> species in the electrolyte to form the anodic film (Equation 1.2). Varying parameters like anodisation time, voltage and electrolyte composition may enhance the formation of porous to nanotubular structures. These were the main parameters studied here. Nevertheless, oxide formed on metal is adhered rather well to the metal (substrate) surface.



Large amount of  $ZrO_2$  is required to be used as photocatalysts. Therefore, using  $ZrO_2$  as a thin film on substrate limits the amount of  $ZrO_2$  used, unless a lot of substrates were used. Besides, Zr foil is not cheap. In this thesis, one Zr foil was anodised for many times and each time, the anodic film was removed as to produce free-standing anodic film in a form of loose flakes. The flakes are shown in Figure 1.1. These flakes were then used to degrade MO dye. The flakes are comprised of nanotubular structure.

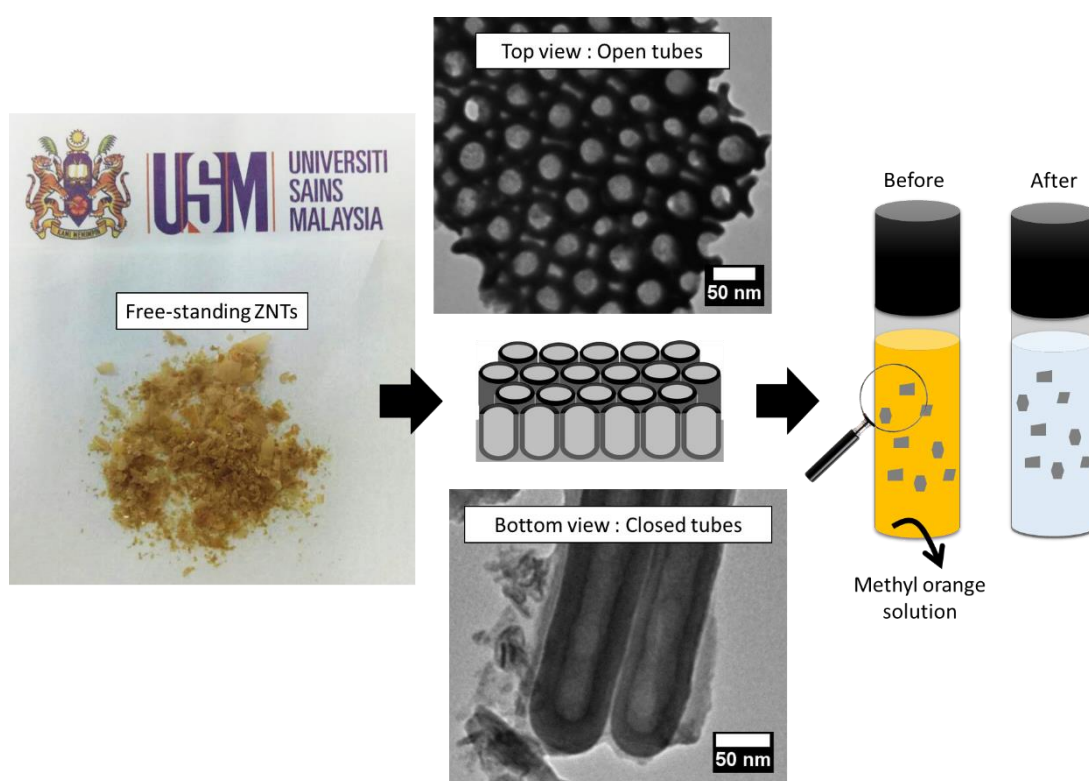


**Figure 1. 1** Overview flow of free-standing ZNTs used in degradation of dye.

In this thesis, a protocol to produce free-standing ZrO<sub>2</sub> is proposed using self-peeling method. Ethylene glycol (EG) was used as anodising electrolyte to produce ZrO<sub>2</sub> nanotubular structure. With the addition of carbonate in the electrolyte, it was observed that the anodic film had a weak adherence to the foil thus the anodic film was easily separated. The separated film forms loose flakes and were used as photocatalyst to degrade MO.

The reasons for the need of free standing as compare to ZNTs film adhered on the surface of Zr foil are:

- i. More ZrO<sub>2</sub> nanotubes can be loaded to react with MO and the amount of catalysts can be exactly measured.
- ii. For ZrO<sub>2</sub> film, there is a possibility of Zr<sup>4+</sup> from Zr substrate to leach and providing secondary pollution during the wastewater treatment process.
- iii. Possibility of using both ends of nanotubes
- iv. Free standing ZNTs which is only few centimetre in length seem practical as it can be sieved out from the solution after treatment process.

## **1.2 Problem Statement**

Synthesis process of nanostructured ZrO<sub>2</sub> powder can be done by hydrothermal, sol-gel and sonochemical methods. However, all of these processes require long processing time and need multiple steps. Sol-gel process for example can take up to 90 hours formation of crystalline ZrO<sub>2</sub> nanoparticles and require many steps such as solution preparation, gel formation, gel drying and calcination.

Anodic process is a faster alternative process with only few hours needed for sample preparation and 3 to 4 hours for annealing process which results in adhered anodic film on zirconium substrate (not loose powder). To produce powdered  $ZrO_2$ , the anodic film must be detached from the substrate. An optimisation of the fabrication process that can yield free-standing  $ZrO_2$  was studied. In this research, anodic process was studied to produce  $ZrO_2$  nanotubes with addition of  $K_2CO_3$  as oxygen provider. Therefore, the free-standing anodic film comprised of nanotubes. It is known that self-organised nanostructure can be achieved by anodic process can be achieved by anodisation of aluminium oxide nanoporous (Lee, Schwirn et al. (2008) and  $TiO_2$  nanotubes (Macák, Tsuchiya et al. (2005) formation.

However, as to the date, there are limited amount of published works on  $ZrO_2$  nanotubes on zirconium. Despite the fact that  $ZrO_2$  is useful ceramic material and used in various engineering applications. Anodisation is a simple synthesis method which consist of anode and cathode electrode with the presence of electrolyte. To produce ordered nanotubes  $ZrO_2$ , Zr metal (foil) can be anodised in an electrolyte containing small amount of fluoride ions.

To date reported works on Zr are mainly focused on finding conditions of anodisation for nanotubes formation with clear morphology and controllable dimensions (Guo, Zhao et al. (2009);Fang, Luo et al. (2013)). Often fluoride salt, glycerol and formamide mixture are used as electrolyte for ZNTs formation (Zhao, Wang et al. (2008)). However, less research have been done to study ethylene glycol (EG) as anodic electrolyte on zirconium even though it has been reported that EG can be used to produce long nanotubes on titanium at a shorter anodisation times (Taib, Kawamura et al. 2016). Faster growth of ZNTs is also expected when EG is used as electrolyte.

Therefore, in this study, EG was used as the anodising electrolyte. However, it is known that oxidant (oxygen ions or hydroxyl ions) are limited in EG. This leads to ejection of  $Zr^{4+}$  but with limited  $O^{2-}$  or  $OH^-$ , solid oxide cannot be formed. Therefore, several types of oxidant were added in EG electrolyte as the oxygen provider to allow for oxide formation. Choice of certain oxidant in EG may also enhance the formation of ZNTs leading to longer tubes formation at shorter time among oxidants used in this study were:  $H_2O$ ,  $H_2O_2$ , and  $K_2CO_3$ . As there is also limited literature on anodisation parameters for ZNTs formation, effect of voltage and times was also studied, systematically.

This thesis also includes the formation of free-standing ZNTs. To yield free-standing ZNTs formed by anodisation must first be removed from the Zr substrate. free-standing ZNTs can be fully utilized without the presence of substrate. For instance to use ZNTs as active material for catalyst, detached oxides are in a form of flakes. The flakes can be used for water treatment via photocatalysis by immersed the flakes in contaminated solution. The flakes were filtered out and reuse. The Zr substrate can be reused to produce more and more free-standing ZNTs. This study focused on optimised condition or a method in which the free-standing ZNTs, comprises of the nanotubes can be removed from the metal Zr substrate on which it has to grow, preferably by a single step process.

To detach the film from the substrate, the adherence between the film and the Zr foil must be weakened. There are many ways to achieve this; scotch tape, reverse bias voltage (Shin and Lee 2009) and immersion process (Fang, Huang et al. 2011). In this study, carbonated electrolyte which can emit carbonaceous gasses during anodisation was found to be efficient in weakening the bond between the film and the foil. The method proposed in this study is termed self-peeling method whereby the



anodic film was found to be easily detached from the substrate. The method is faster and much more effective than any other methods reported. Once the ZNTs film was detached from the Zr substrate, it will be cleaned and annealed. The self-peeling ZNTs were used to degrade MO. Till date, no sufficient work have been done on degradation of MO using free-standing ZNTs. Fang, Luo et al. (2013) reported on 20 % degradation of MO after 2 h when using free-standing ZNTs made in formamide/glycerol electrolyte. However, the rate of oxidation is rather slow.

### **1.3 Objectives**

The focus of this work is to synthesis optimum condition of  $ZrO_2$  nanotubes for enhance its performance in photocatalyst application. Several objectives have been listed to investigate the optimise condition of  $ZrO_2$  nanotubes and their application. The objectives of this work are:

- a) To synthesis and characterise  $ZrO_2$  nanotubes in EG based electrolyte by anodisation process.
- b) To access the parameters of self-peeling of  $ZrO_2$  nanotubes to yield free-standing ZNTs at short period of time by varying oxygen provider.
- c) To evaluate the photocatalytic activity of ZNTs for degradation of methyl orange.

## **1.4 Research scope**

This work is divided into three parts to ensure the objectives can be achieved. The first part highlights the formation of ZrO<sub>2</sub> nanotubes during the anodisation process in several parameters. The parameters investigated are different: concentration of K<sub>2</sub>CO<sub>3</sub> addition, amount of NH<sub>4</sub>F, vol % of K<sub>2</sub>CO<sub>3</sub> addition, anodisation voltage and annealing temperature. After the synthesis process is done, ZrO<sub>2</sub> nanotubes produced were analysed by using several characterisation methods. Besides, the mechanism of self-peeling of ZNTs was proposed to explain the behaviour of ZNTs during the detachment process. Then, the second part of this work focuses on the performance of ZrO<sub>2</sub> nanotubes produced by the anodisation process. Finally, ZrO<sub>2</sub> nanotubes were tested for photocatalytic activity for the degradation of methyl orange.

## **1.5 Outline of thesis**

This thesis consists of five chapters. Chapter 1 gives a brief overview of this work where the introduction, problem statements, objectives and research scope are covered.

Chapter 2 consists of a literature review related to this work. The comparison of methods to synthesise ZrO<sub>2</sub> nanostructures was covered, followed by a literature review of previous researchers on the anodisation method. Properties of ZrO<sub>2</sub> nanotubes were also explained in this section.

Chapter 3 covers the experiment design which included the materials, chemicals and experimental procedures for the anodisation process and photocatalytic study. A brief explanation of characterisation techniques was also included in this chapter.

Chapter 4 presents the experimental results and analysis of this work which is followed by discussion to explain and support the results obtained. Proposed mechanisms were included for further understanding of this work.

Chapter 5 stated the conclusion of this work as well as suggestions and recommendations for further studies.

## **CHAPTER TWO**

### **LITERATURE REVIEW**

#### **2.1 Introduction**

Zirconium Oxide,  $ZrO_2$  or as so-called as zirconia is a ceramic materials that has been widely used in modern industry and engineering fields. To fulfil demand, synthesis protocols are becoming more important for large scale production of  $ZrO_2$ . There are various methods that can be used to result in  $ZrO_2$  of different structures some in nanoscale (nanostructure). In this chapter, general review of several methods to synthesis  $ZrO_2$  nanostructures is presented first. Then, the next part will reviews anodic process and its important parameters as this method was a chosen method for  $ZrO_2$  nanotubes formation in this study. The last part will focus on the behaviour of  $ZrO_2$  nanostructures as catalyst for photocatalytic applications.

#### **2.2 Methods to synthesis $ZrO_2$**

There are several methods that can be used to synthesis of  $ZrO_2$  nanostructures such as hydrothermal, sol-gel, and sonochemical method. These three methods are common methods to produce nanoparticles which with different types of nanostructures depending on the exact condition of synthesis. Noh et al. (2003) used hydrothermal method to synthesis  $ZrO_2$  powder where used zirconyl chloride octahydrate ( $ZrOCl_2 \cdot 8H_2O$ ) was used as precursor with ammonium hydroxide ( $NH_4OH$ ) and potassium hydroxide (KOH) addition. The precursors were aged for 24 h at 100 °C. Then, vacuum-filtered was used to determine the powder by washed with distilled water to completely remove  $Cl^-$  ions and yield  $ZrO_2$  nanoparticles.

Kumari et al. (2009) also synthesis  $ZrO_2$  nanorods using hydrothermal process. They used zirconyl nitrate hydrate ( $ZrO(NO_3)_2 \cdot xH_2O$ ) and sodium hydroxide (NaOH) solution. Both solutions were stirred then sonicated for 30 min to ensure homogenous solution. The mixture was placed in a Teflon-lined autoclaved added with absolute ethanol and was left to operate for 24 to 72 h at  $\sim 250$  °C to get nanorods. Similar work has also reported by Matos et al. (2009) whereby  $ZrO_2$  nanopowder were prepared by  $ZrOCl_2 \cdot 8H_2O$  at 120 °C for 72 – 96 h. It can be concluded that hydrothermal process can produced large amount of  $ZrO_2$  powder but required a very long process.

Sol-gel methods are also equally a long process. A sol-gel process involves the formation of a sol, which is a suspension of solid particles in a liquid, then formation of a gel, which is a diphasic material with a solid encapsulating a liquid. The liquid must then be removed from a gel by drying process to obtain a xerogel or aerogel which then has to be annealed for oxide formation. For example Santos et al. (2008) used sol-gel method by mixing n-propanol, zirconium n-propoxide, acetic acid and deionized water at 70 °C for 28 h. The gel was kept at room temperature for 48 h as to dry it before being subjected to anneal from 200 to 800 °C for 12 h. Total time for processing was almost 88 h.

Another work is by Sreethawong et al. (2013) whereby  $ZrO_2$  nanoparticles were also prepared by sol-gel method but with structure-directing surfactant. Initially, acetylacetone (ACA) was mixed with zirconium (IV) propoxide (ZP) in 1-propanol to obtain mixture ZP/ACA with molar ration 1:1. The mixture was shaken to ensure the solution is homogeneous. 0.1 M laurylamine hydrochloride (LAHC) was prepared to add with ZP/ACA to obtain ZP/LAHC with molar ratio 4:1. Then, ZP/LAHC mixture was aged for a day at 40 °C and followed oven drying for a week at 80 °C to complete the gelation process. The wet was dried at 80 °C for overnight before being calcined

for 4 h at 500 °C to produce ZrO<sub>2</sub> nanoparticles. This process indeed took an extremely long time for nanoparticles formation (~ 10 days).

In recent year, Kumar and Ojha (2015) synthesis ZrO<sub>2</sub> nanoparticles by using sol-gel method where ZrOCl<sub>2</sub>.8H<sub>2</sub>O as the precursor and need to be stir for 1 h. Ammonia solution was added while stirring until the solution in 10 to 12 pH value. Then, the gel solution was dried at 100 °C and grinded to obtain powder form. The powdered samples were calcined at different temperature: 500, 600, 700 and 900 °C for 3 h for the final product. This process consists a lot of steps and take around 6 hours to get the nanoparticles.

Sonochemical process for ZrO<sub>2</sub> nanoparticles formation on the other hand, was reported by Ranjbar et al. (2012) using isophthalic acid-zirconium (IV) nanocomposite. Sonochemical process can be done by placing the precursor solution (zirconyl nitrate pentahydrate, potassium iodide and isophthalic acid in an ultrasonic bath. Chemical reactions and processes occurred when ultrasound was applied. This can translates to faster reaction time. Sonication was done for 30 min for reaction and to ensure homogeneous solution. The ZrO<sub>2</sub> precursor was then calcinated for 4 h at 700 °C to get the ZrO<sub>2</sub> nanoparticles. Faster reaction is observed with sonochemical process.

Sonochemical of zirconyl nitrate solution for nanocrystalline ZrO<sub>2</sub> was also done by Zinatloo-Ajabshir and Salavati-Niasari (2014). Propylenediamine and distilled water were added in with zirconyl nitrate then sonication was done on the mixture at 25 °C. Once a white gel was obtained, process was stopped and the gel was filtered and washed several times before being dried at 80 °C and calcinated at 600 °C for 4 h.

Manoharan et al. (2015) reported on ZrO<sub>2</sub> nanoparticles were formed by sol-gel method and followed by sonication process for formation. Zr-precursor was mixed with oxalic acid and stirred until the gel dissolved and form white solution. The precipitate obtained was added with drops of 10 M ammonia liquid to main the pH solution at 8. Then, zirconium hydroxide precipitate was applied with high intensity ultrasound for 30 min and maintaining the temperature at 25 °C and aged for 12 h. After washed with distilled water and ethanol, the precipitate was dried in hot air oven at 100 °C and calcinated for 2 h at 800 °C to get the final product. This process appears to be longer than direct sonication process and much more complicated.

Based on the three different methods to synthesis ZrO<sub>2</sub> nanostructures, it was concluded that the processes are rather time consuming and hence can be translated to high energy consumption on each steps taken. Moreover, the overall process seems to be complicated and proper care must be taken to ensure minimum contamination.

### **2.3 Anodisation of Zirconium**

In general anodising refers to conversion of zirconium surface to anodic film of ZrO<sub>2</sub>. Anodisation of zirconium can be accomplished in a wide variety of electrolyte since different electrolyte may have different set up of experiment. For example, employing varying operating conditions including concentration and composition of the electrolyte, pH, temperature duration of anodisation and voltage of applied to zirconium are need to be consider as well. In order to produce nanotubular oxide, anodisation parameters need to be optimised.

### 2.3.1 Evolution of ZrO<sub>2</sub> in anodisation process

The first few works on anodisation of Zr for ordered nanoporous anodic film formation was reported by Tsuchiya and Schmuki (2004). They anodised Zr in 1 M H<sub>2</sub>SO<sub>4</sub> containing 0.1 wt % NH<sub>4</sub>F electrolyte for 5 h at different voltages. Based on the observation, only specific area of the surface formed pores at 10 V while for the higher voltages at 20, 30 and 40 V formed regular porous layer. The structures formed exhibit sponge-like structures of ZrO<sub>2</sub> becomes larger when increasing the voltages. This study has been limited up to 50 V since sparking was observed during the anodization process. Hence, applied voltage has been concluded as one important parameter in anodisation process for nanostructured ZrO<sub>2</sub> formation.

Further study was done by Tsuchiya et al. (2005b) by using 0.2 wt% of NaF in 1 M H<sub>2</sub>SO<sub>4</sub> at 20 V. This study discovered three different cases of ZrO<sub>2</sub> formation when three different electrolytes: 1 M H<sub>2</sub>SO<sub>4</sub>, 0.2 wt% of NaF and mixture of 1 M H<sub>2</sub>SO<sub>4</sub> with 0.2 wt% of NaF were used. By using 1 M H<sub>2</sub>SO<sub>4</sub>, only compact anodic oxide was formed. Whereas in 0.2 wt% of NaF electrolyte, porous structures with around 70 nm in diameter was formed but in shorter length of 1 μm. By combining 1 M H<sub>2</sub>SO<sub>4</sub> with 0.2 wt% of NaF as electrolyte, 12 μm in thickness, 50 nm in diameter, anodic film was obtained. Here, the choice of electrolyte is concluded to be a major parameter needed to be considered for the formation of nanoporous anodic ZrO<sub>2</sub> by anodisation process.



Tsuchiya's group reported on the use of 0.5 wt% of  $\text{NH}_4\text{F}$  in 1 M  $(\text{NH}_4)_2\text{SO}_4$  at 20 V for 1 h (Tsuchiya et al. (2005a); Tsuchiya et al. (2005c)) for  $\text{ZrO}_2$ . ZNTs with diameter around 50 nm with 16.6  $\mu\text{m}$  length formation. Only compact oxide layer was in fluoride-free electrolyte. They managed to increase the length of nanotubes but the diameter was  $\sim 50$  nm. From this, the presence of fluoride in electrolyte has been concluded as the major contribution to the formation and growth of  $\text{ZrO}_2$  nanotubes. Figure 2.1 shows the evolution of  $\text{ZrO}_2$  nanostructure from porous to tubular of Tsuchiya's group.

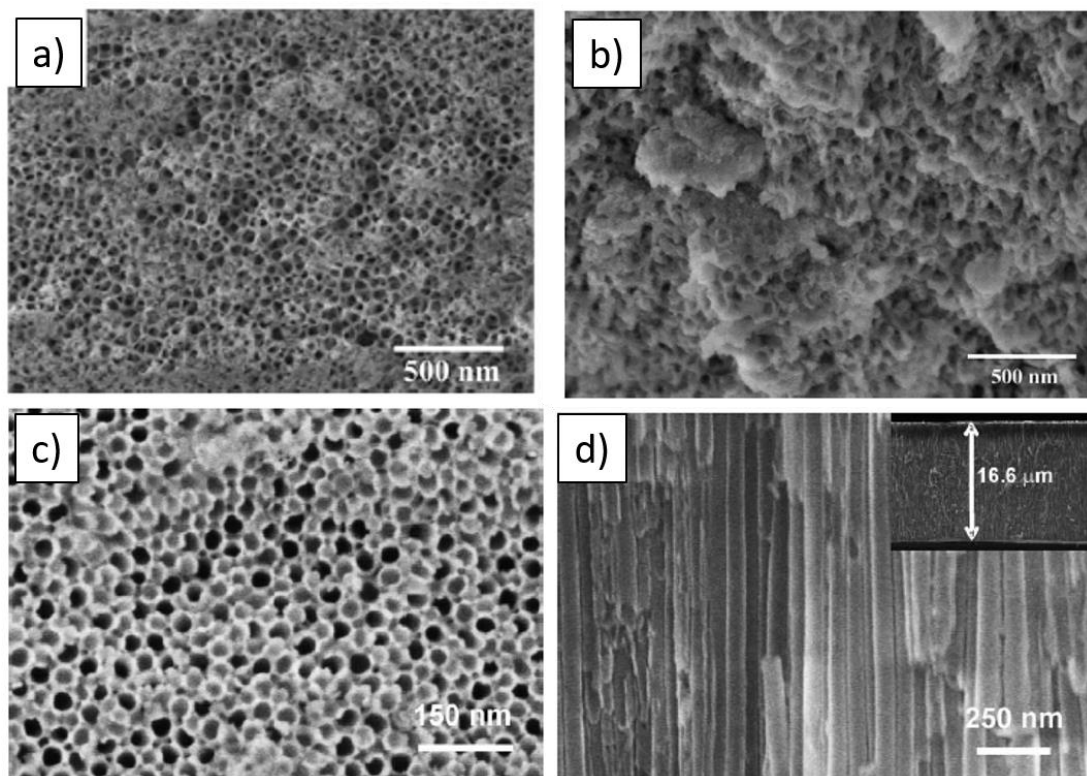


**Figure 2. 1** SEM micrographs of anodised zirconium: a) surface and b) cross-section view of porous structures made in 1 M  $\text{H}_2\text{SO}_4$  / 0.1 wt%  $\text{NH}_4\text{F}$  (Tsuchiya and Schmuki, 2004), c) surface and d) cross-section view of nanotubes structures made in 0.5 wt% of  $\text{NH}_4\text{F}$  in 1 M  $(\text{NH}_4)_2\text{SO}_4$  (Tsuchiya et al., 2005c).

At the same time as Tsuchiya's, Lee and Smyrl (2005) reported on 1  $\mu\text{m}$  long, 20 nm diameter ZNTs. They used 0.5 wt% HF solution, 10 V with duration of 1 to 10 min of anodisation process. Similar to what observed from Tsuchiya's group, Lee and Smyrl concluded that  $\text{F}^-$  ion are crucial for ZNTs formation. Fluoride-free electrolyte only produced compact oxide layer while in the presence of fluoride enhanced the formation of porous structure leading to nanotubular oxide. Lee and Smyrl (2008) continued their work by using 0.5 wt% HF solution at 20 V for 20 min. Similar 20 nm diameter ZNTs with wall thickness of 5 nm were produced. It appears that acidic electrolyte (HF based) has no significant effect on the diameter of ZNTs. To achieve control over diameter and length (dimensions of ZNTs), electrolyte composition was experimented which include the use of organic electrolyte.

Therefore, the next section will focus more on the role of electrolyte on the evolution of  $\text{ZrO}_2$  nanotubes either in controlling the dimensions as well as on ensuring successes in converting pores to tubes. Nevertheless, if to compare anodisation with the three chemical processes mentioned in the previous section, anodisation can be done for only few hours to get the nanostructure desired translating to fast formation using this method..

### **2.3.2 Electrolyte effect on formation of ZNTs**

There is a lot of information from the literature on the effect of electrolyte to the growth of ZNTs. Generally, there are three main outcomes will be the guidelines to determine the growths of ZNTs which are: (i) the success in ZNTs formation, (ii) the growth rate and (iii) control over diameter and length of ZNTs. Few example of electrolyte such as glycerol-based, EG-based and buffered-based electrolyte, are being reviewed in this section. As will become obvious later, reported works on EG-based electrolyte is not as much as glycerol-based electrolyte.

### 2.3.2 (a) Glycerol-based electrolyte

Fabrication of ZNTs in organic electrolyte was first reported by Zhao et al. (2008a) where they used mixture of formamide and glycerol with ratio of 1:1 added with 1 wt%  $\text{NH}_4\text{F}$  and 3 wt% of  $\text{H}_2\text{O}$  for 24 h at 50 V. They managed to produce 190  $\mu\text{m}$  long ZNTs with outer diameter of around 130 nm and wall thickness of 66 nm. This indicated the success in the formation of extremely long nanotubes by anodisation as compared to HF based electrolyte shown previously. They however, observed some loose solid matter covering the mouth of the ZNTs but were to remove them by using ultrasonic rinse. They also reported that by prolonging the anodisation time up to 24 h, the ZNTs can be made very long but with surfaces covered with some precipitates (Zhao et al. (2008a)).

Berger et al. (2008a) introduced two-step anodisation of Zr where the first anodization was done in 1 M  $(\text{NH}_4)_2\text{SO}_4$  containing 0.75 M  $\text{NH}_4\text{F}$  for 30 min at 20 V. Then, the layer obtained was removed by sonication process in ethanol. The second anodization step was conducted in two different electrolytes were 1 M  $(\text{NH}_4)_2\text{SO}_4$  containing 0.15 M  $\text{NH}_4\text{F}$  and ethylene glycol/glycerol (50:50) containing 0.3 M  $\text{NH}_4\text{F}$  and 4 vol%  $\text{H}_2\text{O}$ . The purpose of two-step anodization procedure is to get highly ordered hexagonal structure for ZNTs produced. Berger et al. also tried to compare the formation of ZNTs in aqueous and organic electrolyte. After 1 h anodisation, the length of nanotubes produced in aqueous and organic electrolyte were reported to be 18 and 9  $\mu\text{m}$ , respectively indicating faster growth in aqueous electrolyte. After 3 h the length increases to 25  $\mu\text{m}$  but the tubes collapsed and growth was slow as 40  $\mu\text{m}$  for 24 h anodisation times. This indicated that anodisation electrolyte is an important factor in controlling the length of the nanotubes as well as duration of anodisation (Berger et al. (2008a)).

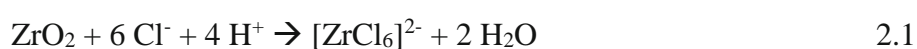
Berger et al. (2008b) also studied the combination of 0.35 M of  $\text{NH}_4\text{F}$  with different amounts of  $\text{H}_2\text{O}$  in glycerol for 1h at 60 V without water, only porous structure was obtained (Berger et al. (2008b)). With the increasing the amount of water added in the organic electrolyte, nanotubes were clearly separated. The transition from porous to tubular surface is therefore concluded to be influenced by water content in glycerol. In 2011, Muratore's group reported on similar electrolyte as reported by Berger et al. (2008 b) where glycerol was added with 1 or 5 vol% of  $\text{H}_2\text{O}$  but different anodic voltage which are 20 and 40 V ((Muratore et al., 2010); (Muratore et al., 2011a); (Muratore et al., 2011b); (Muratore et al., 2011c)). The nanotubes diameter made by Muratores' work slightly smaller compared to Berger's work where they able to get ~ 80 nm. This is due to the different anodic voltage used in both works which high anodic voltage may increase the nanotubes diameter.

Guo et al. (2009c) used formamide and glycerol with ratio of 1:1 with containing 1 wt%  $\text{NH}_4\text{F}$  for 24h at 50 V similar to Zhao et al. (2008a) but with different amount of  $\text{H}_2\text{O}$  (1 wt%) (Guo et al. (2009c), Zhao et al. (2008a)). As reported, they managed to increase diameter up to 350 nm while the length of nanotubes was about ~ 100 nm.

Wang and Luo (2010) investigated the effect of 0.05 M  $(\text{NH}_4)_2\text{HPO}_4$  in glycerol containing 5 vol%  $\text{H}_2\text{O}$  and 0.35 M  $\text{NH}_4\text{F}$ . 75 nm diameter ZNTs were produced. They further investigated on anodisation without the presence of phosphate but at different anodisation time and voltage ((Wang and Luo, 2011a); (Wang and Luo, 2011b)). The maximum diameter that can be obtained was 50 nm with length of 13  $\mu\text{m}$ . The existence of  $(\text{NH}_4)_2\text{HPO}_4$  did not really effect the growth of ZNTs (Wang and Luo (2010)).

Zhao et al. (2012) did a comparative study by anodising zirconium in formamide and glycerol added with either 2 wt% HCl / 3.5 wt% H<sub>2</sub>O or 1 wt% NH<sub>4</sub>F / 3 wt% H<sub>2</sub>O (Zhao et al. (2012)). ZNTs were successfully formed in both electrolytes with tube closed at the bottom part (metal|oxide interface). They observed that in the presence of HCl, the ZNTs were easily detached from the substrate as the electrolyte dissolved the bottom part of the nanotubes forming “loose” bottom. When NH<sub>4</sub>F/H<sub>2</sub>O added formamide and glycerol was used, the bottom part of ZNTs seems to be thinner than the wall of the nanotubes. The electrolytes have therefore concluded to have a great impact on the morphology of nanotube bottom whereby dissolution occurred in the nanotubes here is the highest. They described on the influence of electrolyte temperature (thermal conductivity and mass transfer) on the dissolution of oxide at the bottom part of the nanotubes. Higher temperature and faster mass transfer velocity would accelerate the dissolution of oxides.

Apart from fluoride, there are also works in the literature that addressed on the importance of chloride on the formation of porous or nanotubular oxide on zirconium. Guo et al. (2009a) experimented on HCl in formamide and glycerol (ratio 1:1) with containing 3.5 wt% of H<sub>2</sub>O in anodization for 5h at 20 V (Guo et al. (2009a)). In this study shows the transformation of knob structure (0.5 wt%) to cabbage-like surface morphology (5 wt%) when increasing the amount of HCl was added in the electrolyte. Here, they introduced Cl<sup>-</sup> ions in the solution which play the same role as the F<sup>-</sup> ion in other studies as the chemical dissolution to happen. The reaction can be describe as below:



Xu et al. (2012) used glycerol with 5 vol% of H<sub>2</sub>O for different molarity of NH<sub>4</sub>F which are 0.1, 0.5, 0.7 and 1.1 M. They managed to get 90 to 130 nm in diameter of nanotubes as the increasing molarity of NH<sub>4</sub>F. Interesting results was observed for the length of nanotubes where it increase from 4 to 10 μm for 0.1 and 0.5 M of NH<sub>4</sub>F. While used 0.7 M of NH<sub>4</sub>F addition, the nanotubes length were decreased to 6 to 7 μm (Xu et al. (2012)). Therefore, addition NH<sub>4</sub>F in anodic electrolyte might increase the length of nanotubes but it may reduce the length when it achieved the optimum value due to the excess chemical etching condition.

Fang et al. (2011) used mixture of formamide and glycerol with ratio 1:1 containing 1 wt% NH<sub>4</sub>F and 3 wt% H<sub>2</sub>O at 50 V for 3h and managed to get around 30 μm of thickness and about 60 nm tube diameter. They also investigated the same electrolyte with two-step anodisation method but it seems that the dimension of ZNTs not improved since they only get the same results (Fang et al. (2012a); Fang et al. (2012b)). Fang et al. (2013) varies the anodic voltage which are 20, 30, 40, and 50, managed to get nanotube diameter about 58, 80, 91 and 115 nm, respectively. They also reported on producing free-standing membrane of ZNTs and will be explain in the next section.

Hosseini et al. (2015) used mixture of glycerol and DMF with ratio 1 to 1 and addition of 1 wt% NH<sub>4</sub>F and 3 wt% H<sub>2</sub>O as the anodic electrolyte. They varies the anodic voltage which are 20, 50 and 60, manage to get diameter approximately 40, 150 and 160 nm, respectively. Then they work on varying anodic temperature which 5, 23 and 35 ° C, able to get diameter approximately 12, 150 and 210, respectively (Hosseini et al. (2015)). As the conclusion, increasing anodic voltage will increase the nanotubes diameter and room temperature might be the suitable temperature for this anodization electrolyte.

Hosseini et al. (2016) also work on mixture of glycerol and DMF with ratio 1 to 1 with varying the amount of  $\text{NH}_4\text{F}$  and  $\text{H}_2\text{O}$  at 50 V for 3 h. They prepared two sets of experiment which first, 1 wt%  $\text{NH}_4\text{F}$  with 1, 3 and 5 wt%  $\text{H}_2\text{O}$ , and second, 3 wt%  $\text{H}_2\text{O}$  with 0.5, 1 and 2 wt%  $\text{NH}_4\text{F}$ . The average diameters of ZNTs produced in 1, 3 and 5 wt%  $\text{H}_2\text{O}$  are 30, 40 and 55 nm, respectively while in 0.5, 1 and 2 wt%  $\text{NH}_4\text{F}$  are 20, 40 and 80, respectively (Hosseini et al. (2016)). Therefore, addition of  $\text{NH}_4\text{F}$  and  $\text{H}_2\text{O}$  affect the increasing dimension of ZNTs produced.

### **2.3.2 (b) Ethylene Glycol based electrolyte**

Not much work have been reported on using EG as the anodic electrolyte. Li et al. (2011) used two-step anodization process. This study has started to use 100 ml of ethylene glycol (EG) with 17.5 wt. %  $\text{NH}_4\text{F}$ . For the first anodisation step, they used sweep rate of  $1 \text{ V s}^{-1}$  for potential sweep from 0 to 30 V and remain at 30 V for 30 min. After first anodization step, the anodic layer was removed by sonication process in ethanol for 15 min. Followed by the second anodization step, the conditions was remain like previous but only for 5 min. The range of diameter that reported in this study about 26 to 36 nm while the length of nanotube is around 2.3  $\mu\text{m}$ .

Pisarek et al. (2014) work on using EG by adding 0.38 wt%  $\text{NH}_4\text{F}$  with  $\text{H}_2\text{O}$  at 40 V for 1.5 h. About 55 nm in diameter with length range 500 to 650 nm was obtained. Chen et al. (2015) also reported on EG electrolyte with addition of 0.25 wt%  $\text{NH}_4\text{F}$  with 1 vol%  $\text{H}_2\text{O}$  for 45 V but they done the experiment with two-step anodiaation method. Here, they able to get longer nanotubes compared to previous works which around 10  $\mu\text{m}$  while the nanotubes diameter is around 10 nm only. Based on this two works, we can clarify that few modification of electrolyte composition and anodization condition may improve the dimension of nanotubes produce by anodic process.

Synthesizing of ZNTs was continued by using mixture of 99 ml EG with 0.3 wt%  $\text{NH}_4\text{F}$  and 1 ml of 1 M  $\text{K}_2\text{CO}_3$  addition for 1 h (Bashirom et al. (2016a); Bashirom et al. (2017)). They varies the anodic voltage with range 20 to 60 V. Here, they managed to get 70 nm in diameter and 10  $\mu\text{m}$  in length at 60 V. Bashirom et al. (2016b) continued their work in mixture of EG and  $\text{NH}_4\text{F}$  with by comparing addition of  $\text{H}_2\text{O}$  with  $\text{H}_2\text{O}_2$  and  $\text{NH}_4\text{F}$  with  $\text{NH}_4\text{Cl}$ . When perform the electrolyte with addition of  $\text{NH}_4\text{F}$  in  $\text{H}_2\text{O}$  with  $\text{H}_2\text{O}_2$ , they able to get diameter range 25 to 30 nm with length about 4  $\mu\text{m}$ . While when  $\text{NH}_4\text{Cl}$  added into electrolyte with  $\text{H}_2\text{O}$  with  $\text{H}_2\text{O}_2$ , volcanical knobs were observed instead of formation of nanotubes. Therefore, the presence of  $\text{F}^-$  and  $\text{Cl}^-$  ions might be the reason why the transformation between nanotubes with volcanical knob.

### **2.3.2 (c) Buffered electrolyte**

Buffered electrolyte (aqueous) works were also reported in literature which used  $\text{Na}_2\text{SO}_4$  and  $(\text{NH}_4)_2\text{SO}_4$  can increase high aspect ratio of the nanotubes itself. These electrolytes can be made acidic by adding in acid like HF or  $\text{H}_2\text{SO}_4$ . Guo et al. (2009b) studied the similar electrolyte as reported by Tsuchiya et al. (2005a) and Tsuchiya et al. (2005c) which is 1 M  $(\text{NH}_4)_2\text{SO}_4$  with 0.5 wt% of  $\text{NH}_4\text{F}$  at 20 V but they anodised the Zr for 3 h. Similar result was observed for diameter of nanotube which is around 50 nm while they managed to increase the length up to 20  $\mu\text{m}$ .

Ismail et al. (2011) reported on the use 1 M  $\text{Na}_2\text{SO}_4$  with 0.5 wt. % of  $\text{NH}_4\text{F}$  at 20 and 50 V for 1 h. They managed to increase the diameter of ZNTs up to 50 nm while the length of nanotubes was around 6  $\mu\text{m}$  when using higher voltage. Growth in  $\text{Na}_2\text{SO}_4$  appears to be rather slow whereby ZNTs formed were rather short.



Stepień et al. (2014) compared the different between anodised in inorganic and organic electrolyte. Inorganic electrolyte used was 0.1 M HF with 0.5 M Na<sub>2</sub>SO<sub>4</sub> and organic electrolyte was glycerol added with 0.1 M HF with 0.5 M Na<sub>2</sub>SO<sub>4</sub> as well. Anodisation in inorganic electrolyte resulted in ZNTs with diameter range 40 to 80 nm depending on anodisation voltage. The length of ZNTs was linearly increase with anodization time up to 5 h which around 30 µm. above 5 h, the ZNTs started to collapse. This is longer than Ismail et al's ZNTs and hence it can be concluded that the existence of HF may have influenced the rate of formation. Moreover, with HF addition, there is a possibility of pH alteration which induce more rapid growth of the ZNTs.

In organic electrolyte, Stepień et al. (2014) used only 20 V as anodisation voltage, but they varied glycerol content. However, glycerol appeared to have a negative effect on the ZNTs growth. The addition of glycerol in the electrolyte slowed the rate of ZNTs formation.

Work on (NH<sub>4</sub>)<sub>2</sub>SO<sub>4</sub> as electrolyte has been reported by Frandsen et al. (2011). Two-step anodisation process was done whereby first anodization was performed in 0.75 M NH<sub>4</sub>F with 1 M (NH<sub>4</sub>)<sub>2</sub>SO<sub>4</sub> for 15 min at 20 V. After the first anodized layer was removed by using adhesive tape, second anodisation step was performed 0.15 M NH<sub>4</sub>F with 1 M (NH<sub>4</sub>)<sub>2</sub>SO<sub>4</sub> for 15 min at 20 V. Since the anodisation was done in two-step, well aligned nanotubes with highly order were obtained with length of 10 µm and pores diameter 40 nm. Zhang and Han (2011) also used 1 M (NH<sub>4</sub>)<sub>2</sub>SO<sub>4</sub> with 0.15 M NH<sub>4</sub>F at 20 V for 1 h. They able to get ~ 65 nm diameter ZNTs, but only 7 µm in length. This is similar to Na<sub>2</sub>SO<sub>4</sub>'s work as well as one step process. There are therefore much to be explored in term of two step anodisation process for ZNT's formation.